



Conserved mechanism for vacuolar magnesium sequestration in yeast and plant cells

Ren-Jie Tang^{1,4}, Su-Fang Meng^{2,4}, Xiao-Jiang Zheng^{1,3,4}, Bin Zhang^{© 2,3,4}, Yang Yang², Chao Wang^{1,3}, Ai-Gen Fu³, Fu-Geng Zhao², Wen-Zhi Lan² and Sheng Luan ^{© 1} □

Magnesium (Mg^{2+}) is an essential nutrient for all life forms. In fungal and plant cells, the majority of Mg^{2+} is stored in the vacuole but mechanisms for Mg^{2+} transport into the vacuolar store are not fully understood. Here we demonstrate that members of ancient conserved domain proteins (ACDPs) from *Saccharomyces cerevisiae* and *Arabidopsis thaliana* function in vacuolar Mg^{2+} sequestration that enables plant and yeast cells to cope with high levels of external Mg^{2+} . We show that the yeast genome (as well as other fungal genomes) harbour a single ACDP homologue, referred to as MAM3, that functions specifically in vacuolar Mg^{2+} accumulation and is essential for tolerance to high Mg. In parallel, vacuolar ACDP homologues were identified from *Arabidopsis* and shown to complement the yeast mutant $mam3\Delta$. An *Arabidopsis* mutant lacking one of the vacuolar ACDP homologues displayed hypersensitivity to high-Mg conditions and accumulated less Mg in the vacuole compared with the wild type. Taken together, our results suggest that conserved transporters mediate vacuolar Mg^{2+} sequestration in fungal and plant cells to maintain cellular Mg^{2+} homeostasis in response to fluctuating Mg^{2+} levels in the environment.

ineral nutrients enter the cell typically in the ionic form through transporters across the plasma membrane, and shuttle between organelles and cytosol to support biochemical reactions. In fungal and plant cells, a large proportion of minerals is stored in the vacuole that plays an essential role in buffering large variations in environmental nutrient status^{1,2}. When external nutrients are plentiful, excessive nutrients are sequestered into the vacuole, preventing toxicity caused by imbalance among various minerals. When facing nutrient-deficient environments, nutrients stored in the vacuole are remobilized to support cellular metabolism³. Therefore, the vacuolar membrane (tonoplast) harbours a large array of transport proteins that mediate fluxes of minerals into and out of the storage compartment in response to metabolic demands and external nutrient fluctuations^{4,5}.

Magnesium (Mg2+) is an essential mineral nutrient in all life forms. In photosynthetic plant cells, Mg2+ is particularly important because it serves as the core metal of chlorophylls and is an essential cofactor for a number of photosynthetic enzymes⁶. As the most abundant free divalent cation in the cytoplasm, the bulk of Mg²⁺ in fungal and plant cells is stored in the vacuole^{7,8}, stabilizing a cytosolic Mg²⁺ level less than one-tenth of the total Mg in the vacuole^{2,9}. When external Mg²⁺ is high, excessive Mg²⁺ is sequestered into the vacuole to detoxify the cytoplasm. Such a vacuolar pool will be retrieved in fungi or plants when they encounter Mg²⁺ deficiency in the environment. Therefore, the vacuolar sequestration mechanism is critical for both fungi and plants in coping with fluctuating Mg2+ levels in the environment. A particular concern of agricultural and ecological importance is 'serpentine soil', with high Mg²⁺ levels toxic to most plants¹⁰. Although vacuolar Mg²⁺ sequestration is believed to be a critical mechanism for tolerance to high Mg¹¹, the transport proteins involved remain elusive. Earlier studies favour a proton (H⁺)-driven transport model for Mg²⁺ entry into the vacuole, because Mg2+/H+ exchanger activity was detected

in tonoplast vesicles isolated from plant tissues and yeast cells^{12,13}. A gene encoding a Mg²⁺/H⁺ exchanger (MHX) was later identified in Arabidopsis14, but such MHX homologues have not been found in yeast or other fungi. Either knockout or overexpression of AtMHX failed to alter Mg²⁺ accumulation or high-Mg tolerance in plants11,14, suggesting that other Mg2+ transporters are involved in Mg²⁺ delivery into the vacuole to cope with high-Mg toxicity. Potential candidates include CorA-type Mg2+ transporters that were originally identified from bacteria and later found in all eukaryotes including fungi, plants and animals. Budding yeast possesses several CorA homologues that contribute to cellular Mg2+ homeostasis. While plasma membrane-localized ALR1 and ALR2 mediate Mg²⁺ uptake into the cell¹⁵, MRS2 is targeted to the mitochondrial inner membrane and is responsible for Mg2+ influx into the mitochondrial matrix¹⁶. Interestingly, another CorA homologue, MNR2, resides in the vacuolar membrane and functions in Mg2+ remobilization from the vacuolar store, helping yeast cells survive under low extracellular Mg²⁺ levels¹⁷. A family of CorA-like proteins have also been identified as plant Mg²⁺ transporters (MGTs) or homologues of the yeast MRS2 protein (MRS2s) in Arabidopsis^{18,19}. Members of the plant MGT family exhibit Mg²⁺ transport activity and function in a number of processes in plants^{20–22}. In the context of vacuolar transport, one report suggested that MGT2 and MGT3 may play a role in controlling Mg²⁺ accumulation in mesophyll cell vacuoles²³. However, mutants lacking these MGT members grew like the wild type under high Mg2+11, excluding a role for these two MGTs in high-Mg tolerance.

In animal cells, several types of transport protein, in addition to CorA homologues, function in Mg²⁺ homeostasis. Among these, one family belongs to the 'ancient conserved domain proteins' (ACDPs), also known as cyclin M-type divalent metal cation transport mediators (CNNM) in mammals²⁴. This family of proteins features a 'domain of unknown function 21' (DUF21)

¹Department of Plant and Microbial Biology, University of California, Berkeley, CA, USA. ²Nanjing University-Nanjing Forestry University Joint Institute for Plant Molecular Biology, State Key Laboratory for Pharmaceutical Biotechnology, College of Life Sciences, Nanjing University, Nanjing, China. ³College of Life Sciences, Northwest University, Xi'an, China. ⁴These authors contributed equally: Ren-Jie Tang, Su-Fang Meng, Xiao-Jiang Zheng, Bin Zhang. [™]e-mail: lanw@nju.edu.cn; sluan@berkeley.edu

that spans the membrane three or four times, followed by two cystathionine-β-synthase (CBS) domains in the cytoplasmic region²⁵ that may serve regulatory functions²⁶. Of particular relevance is the correlation between hypomagnesaemia and the occurrence of mutations in the gene CNNM2, suggesting that human ACDP/CNNM proteins are involved in Mg²⁺ transport²⁷. Indeed, CNNM1, CNNM2 and CNNM4 exhibit Mg²⁺ efflux activity when overexpressed in human embryonic kidney cells²⁶. Consistently, disruption of CNNM4 function leads to elevation of cellular Mg²⁺ concentration, implicating CNNM4 in Mg2+ efflux across the plasma membrane²⁸. Further support for ACDP proteins acting as Mg²⁺ efflux transporters comes from a study in the pathogenic bacterium Staphylococcus aureus, where an ACDP homologue was identified as 'magnesium protection factor A' (MpfA) that protects bacterial cells from high-Mg²⁺ toxicity, presumably through extrusion of excessive Mg²⁺ out of the cell²⁹. In both fungi and plants, ACDP-like proteins are also present³⁰ but their potential role related to Mg²⁺ transport remains unknown. In this study, we demonstrate that some ACDP homologues from yeast and Arabidopsis are localized to the tonoplast and are required for Mg²⁺ transport into the vacuole. Such vacuolar Mg2+ sequestration mediated by ACDP-type transporters is not only essential for cellular Mg²⁺ accumulation and homeostasis, but is also critical to the survival of both fungi and plants when facing high environmental Mg²⁺ levels.

Results

MAM3 is required for vacuolar Mg²⁺ sequestration in yeast. No previously identified Mg2+ transporter has conferred high-Mg tolerance in fungal or plant cells. In an attempt to identify Mg2+ transporters that play such a role, we surveyed transmembrane proteins in Saccharomyces cerevisiae with homology to a variety of putative Mg²⁺ transport proteins in mammalian cells³¹. One candidate of interest, originally named MAM3, shares low sequence homology but high structural similarity with human ACDP/CNNM proteins that facilitate Mg²⁺ transport in renal cells³². The protein MAM3 is localized specifically to the yeast vacuolar membrane, and knockout of the gene MAM3 led to tolerance to toxic levels of manganese (Mn²⁺)³³. However, MAM3 contributes neither to cellular Mn²⁺ homeostasis nor Mn2+ trafficking in yeast33. In light of studies on human ACDPs that appear to function in Mg²⁺ transport, we reasoned that MAM3 might also function in Mg2+ transport and that the high-Mn-tolerance phenotype of strain mam3∆ might result from antagonism between Mn2+ and Mg2+. To test this idea, we engineered a MAM3 deletion mutant (mam3 Δ) in the background of a haploid S. cerevisiae strain (BY4741), followed by phenotyping of wild-type and mutant cells on medium supplemented with 5 mM Mn²⁺ plus various concentrations of Mg²⁺ or Ca²⁺. Consistent with a previous report, mam 3Δ displayed stronger tolerance to 5 mM Mn²⁺ as compared to the wild type (Supplementary Fig. 1a). Interestingly, low levels of Mg²⁺ in the medium aggravated Mn²⁺ toxicity to both wild-type and $mam3\Delta$ strains, whereas elevated Mg²⁺ concentrations in the medium enhanced high-Mn tolerance in the wild-type strain but not in the $mam3\Delta$ mutant (Supplementary Fig. 1a). In contrast, varying Ca²⁺ concentrations (0.01–10 mM) in the medium did not alter Mn²⁺ tolerance of $mam3\Delta$ relative to wild type (Supplementary Fig. 1a). These results support the hypothesis that MAM3 may control cellular Mg²⁺ levels, thereby altering Mn²⁺ toxicity in yeast cells. Moreover, $mam3\Delta$ showed a cobalt (Co²⁺)-tolerant phenotype that was also modified by external Mg²⁺ levels, but not by Ca²⁺ levels (Supplementary Fig. 1b), corroborating the notion that MAM3 may be directly involved in Mg²⁺ homeostasis that, in turn, affects tolerance to heavy metal ions.

To understand how ion homeostasis is affected by loss of function of MAM3, we compared metal profiles of wild-type and $mam3\Delta$ cells grown in a modified synthetic complete (SC) medium. We found a dramatically reduced Mg content in mutant cells (Fig. 1a),

suggesting that MAM3 plays a major role in Mg^{2+} accumulation. In parallel, a handful of other cations, including K, Ca, Zn and Mn, were slightly elevated in the $mam3\Delta$ mutant, probably to compensate for the loss of Mg. We then monitored the growth of $mam3\Delta$ and wild-type strains on YPD medium supplemented with a variety of excessive divalent cations. While $mam3\Delta$ displayed greater tolerance to Mn^{2+} and Co^{2+} , this strain was specifically hypersensitive to high Mg^{2+} (Supplementary Fig. 2) whereas it grew like the wild type on YPD medium containing similar levels of other cations or sorbitol, which would trigger similar ionic or osmotic stress (Fig. 1b). Because MAM3 is exclusively localized to the vacuolar membrane 33 , these data suggest that MAM3 functions as a tonoplast transporter that detoxifies excessive Mg^{2+} in the yeast cell via vacuolar sequestration.

We next constructed a $mnr2\Delta$ mam3 Δ double mutant to further dissect the role of MAM3 in vacuolar Mg2+ transport. MNR2 is a CorA-type tonoplast Mg2+ transporter that mediates Mg2+ efflux from the vacuolar lumen to the cytoplasm¹⁷. Lack of this transporter in strain $mnr2\Delta$ causes hypersensitivity to high levels of Mn²⁺ (Fig. 1c), a phenotype opposite to that of $mam3\Delta$, supporting the idea that MNR2 and MAM3 mediate opposite fluxes of Mg²⁺ across the tonoplast. If both influx and efflux transporters are deleted, the double mutant should phenocopy the single mutant defective in vacuolar Mg²⁺ influx because Mg²⁺ accumulation into the vacuole occurs earlier and is a prerequisite for the retrieval process. Indeed, MAM3 was epistatic to MNR2 because the double mutant mnr2Δ mam3Δ was hypersensitive to Mg2+ but more tolerant to Mn2+, typically observed in strain $mam3\Delta$ (Fig. 1c). Consistently, while $mnr2\Delta$ overaccumulated Mg in yeast cells, the $mnr2\Delta mam3\Delta$ double mutant, like the mam 3Δ single mutant, retained much less Mg as compared to the wild-type strain (Fig. 1d). These data strongly support the conclusion that MAM3 transports Mg²⁺ into the vacuole, opposite to the function of MNR2 that transports Mg²⁺ out.

Identification of plant 'magnesium release' transporters. Using yeast MAM3 sequence as a query, we identified nine homologues in the Arabidopsis thaliana genome. These nine proteins all contain a DUF21 domain with three to five predicted transmembrane helices followed by a pair of CBS domains in the C-terminal region (Fig. 2a), reminiscent of the structures of yeast MAM3 and human CNNMs. (Supplementary Fig. 3). Because these plant transporters may potentially mediate Mg2+ release from the cytoplasm to either the vacuole (as MAM3 in yeast) or the extracellular space (like CNNMs in human), we named this family MaGnesium Release (MGR) and, accordingly, MGR1-9 in *Arabidopsis* (Fig. 2b). We constructed a phylogenetic tree comparing 88 sequences from ten plant and nine fungal species, as well as their prokaryotic and mammalian relatives (Fig. 2c). In all fungal species analysed, a single gene was present in each genome; however, extensive gene duplication events occurred in plants. Although the green alga Chlamydomonas reinhardtii appeared to contain five homologues clustered into a single and unique group, all land plants from moss to angiosperm evolved multiple MGRs distributed in three different clades, among which clade I was positioned closest to the fungal homologues in the tree. Clade II represented another branch with slightly more members than clade I, while clade III was distant from the other two plant clades but more closely associated with prokaryotic homologues.

We next examined the subcellular localization of the nine *Arabidopsis* MGRs in transiently transformed protoplasts, and found that MGR1, MGR2 and MGR3, like MAM3 in yeast, were localized to the tonoplast (Supplementary Fig. 4 and Fig. 3a,b), consistent with a proteomic study that identified MGR1 and MRG2 as tonoplast proteins³⁴. Clade II members MGR4, MGR5, MGR6 and MGR7 were all targeted to the plasma membrane (Supplementary Fig. 4), while MGR8 and MGR9 were found to reside within the chloroplast (Supplementary Fig. 4).

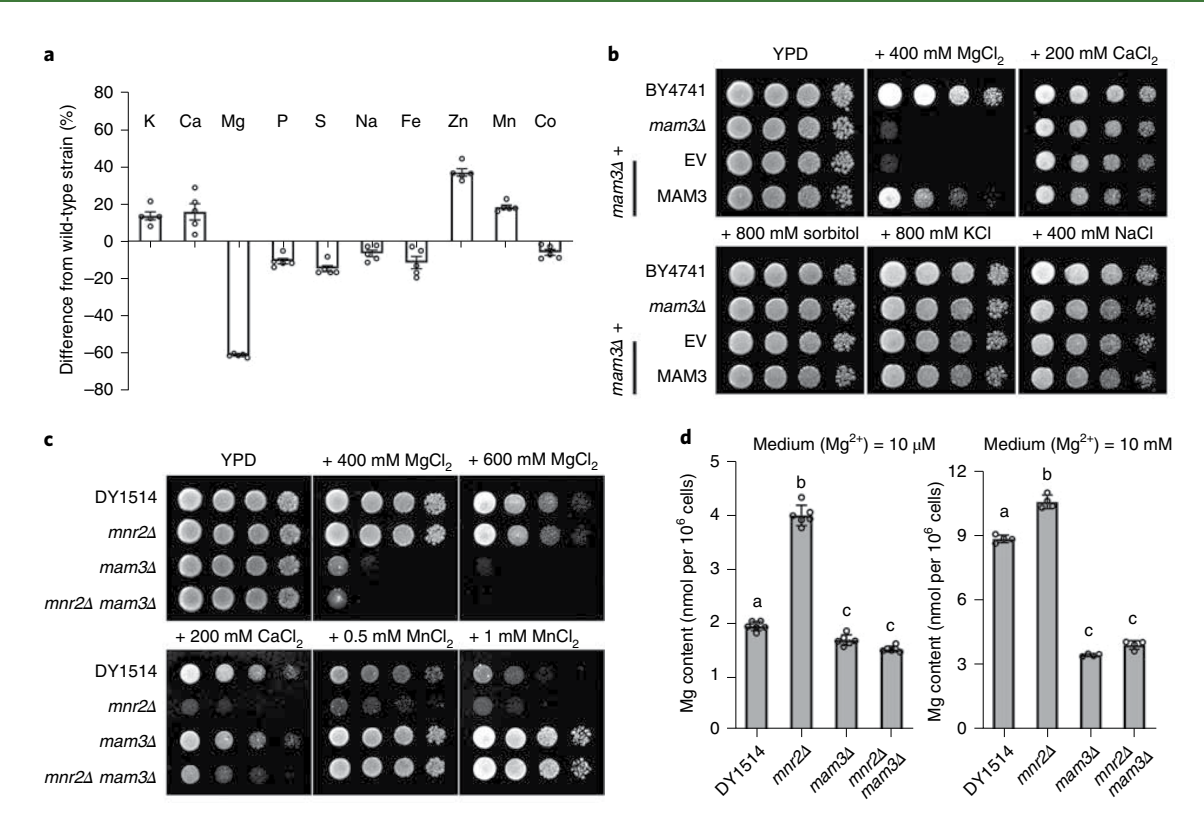


Fig. 1 | MAM3 is required for Mg²⁺ homeostasis and high-Mg tolerance in *S. cerevisiae*. **a**, lonic profiles of wild-type (BY4741) and $mam3\Delta$ strains. For each element, the average value in BY4741 was used as the baseline and differences in $mam3\Delta$ were calculated as percentage increases or decreases. Data represent means ± s.e.m. of five biological replicates. **b**, Hypersensitivity of the $mam3\Delta$ mutant strain to high levels of Mg²⁺. Yeast cells of indicated genotypes were initially grown overnight in liquid YPD medium. EV, empty vector. With a culture at OD₆₀₀ = 1.0, 3 μl of serial decimal dilutions was spotted onto either agar-solidified YPD medium or YPD medium supplemented with 400 mM MgCl₂, 200 mM CaCl₂, 800 mM sorbitol, 800 mM KCl or 400 mM NaCl. Each experiment was repeated using six independent clones, with similar results. **c**, Phenotype of the yeast $mnr2\Delta$ $mam3\Delta$ double mutant. With an OD₆₀₀ = 1.0 culture, 3 μl of serial decimal dilutions were spotted onto YPD medium or YPD medium supplemented with 400 mM MgCl₂, 600 mM MgCl₂, 200 mM CaCl₂, 0.5 mM MnCl₂ or 1 mM MnCl₂. Plate cultures were incubated at 28 °C and photographed after 3 d. Each experiment was repeated using six independent clones with similar results. **d**, Total cellular Mg content of wild-type (DY1514), $mnr2\Delta$, $mam3\Delta$ and $mnr2\Delta$ $mam3\Delta$ strains. Yeast cultures were grown in liquid SC medium containing either 10 μM (left) or 10 mM (right) Mg²⁺, and cell-associated Mg content was analysed using ICP-OES. Data represent means ± s.d. from six independent replicates for yeast cells grown in the presence of 10 μM Mg²⁺, and from four independent replicates for those grown in the presence of 10 mM Mg²⁺. Statistical analyses between groups was performed by one-way analysis of variance followed by Tukey's multiple comparison test. Different letters indicate significant statistical differences at P < 0.01.

To corroborate tonoplast localization of the three vacuolar members, the subject of this study, we generated transgenic *Arabidopsis* plants expressing fusions MGR1–GFP, MGR2–GFP and MGR3–GFP. We again observed fluorescence signals specifically associated with tonoplast in mesophyll protoplasts from these transgenic plants. Such fluorescence signal lit up tonoplast in purified vacuoles from mesophyll cells, demonstrating that MGR1, MGR2 and MGR3 are tonoplast-localized proteins (Supplementary Fig. 5).

Functional analysis of plant vacuolar MGRs in a yeast model. Taking advantage of our new finding that MAM3 functions as a Mg^{2+} transporter required for vacuolar Mg^{2+} sequestration in the yeast cell, we employed genetic complementation of $mam3\Delta$ to address the function of vacuolar MGRs from Arabidopsis. Expression of MGR1 in $mam3\Delta$ effectively rescued its growth defect under high-Mg conditions, to a similar degree as expression of yeast MAM3 (Fig. 4a and Supplementary Fig. 6). Both MGR1 and MAM3 also suppressed high-Mn and high-Co tolerance of $mam3\Delta$ (Supplementary Fig. 7). Furthermore, Mg content in yeast mutant cells was restored to the wild-type level (Fig. 4b), suggesting that MGR1 is competent for Mg^{2+} sequestration into the yeast vacuole to detoxify excess Mg^{2+} . We also expressed several other Mg^{2+} transporters in the $mam3\Delta$ strain and found that, besides MGR1, vacuolar

homologues MGR2 and MGR3, but neither MGTs nor MHX, substituted for MAM3 in regard to vacuolar Mg^{2+} accumulation and detoxification (Fig. 4). These data suggest that plant vacuolar MGRs, like MAM3 in fungi, function in Mg^{2+} sequestration into the vacuolar lumen.

Arabidopsis MGR1 is required for high-Mg tolerance and Mg²⁺ accumulation. To assess the function of the three tonoplast MGR members in *Arabidopsis*, we analysed their expression pattern and found that *MGR1*, *MGR2* and *MGR3* were ubiquitously expressed, but stronger expression was detected in above-ground tissues than in roots (Fig. 3d and Supplementary Fig. 8a). We also analysed their expression in response to different Mg²⁺ levels but did not detect any changes (Fig. 3e and Supplementary Fig. 8b,c). We further generated transgenic *Arabidopsis* plants expressing a *MGR1* promoter-driven β-glucuronidase (GUS) reporter and detected high GUS activity in aerial tissues at various developmental stages (Fig. 3c). In root, *MGR1-GUS* expression was mainly observed in the vasculature whereas a more ubiquitous pattern was present in above-ground organs such as rosette leaf, flower and silique (Fig. 3c).

We isolated transfer DNA insertional mutants for the three MGRs and analysed their phenotypes in the context of Mg²⁺ homeostasis. While mutant *mgr1* was extremely sensitive to high

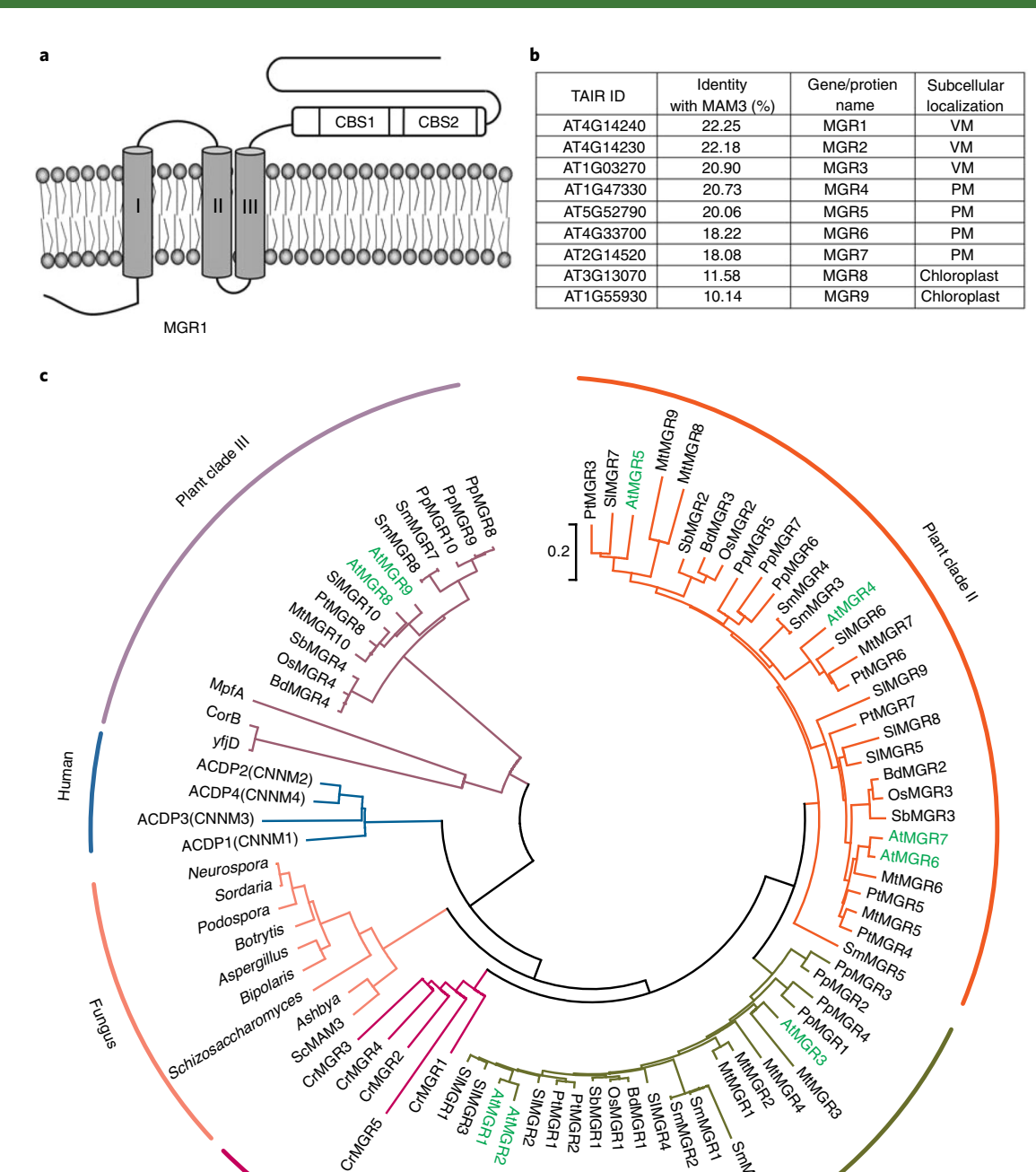


Fig. 2 | Identification and phylogenetic analysis of ACDP homologues in plants. a, Topological model of *Arabidopsis* MGR1 transporter. Three putative transmembrane helixes (I, II, III) predicted by the TMHMM2 v.2.0 programme and a pair of CBS domains are indicated in the boxes of the C terminus. b, Inventory of all ACDP homologues in *A. thaliana*. MGR1-9 were designated based on the degree (from high to low) of sequence identity with yeast MAM3. Gene IDs are listed according to TAIR. The subcellular localization of each protein is given based on the data presented in Supplementary Fig. 4. PM, plasma membrane; VM, vacuolar membrane. c, Phylogenetic analysis of plant, fungal, bacterial and animal ACDP proteins. Homologues of ACDP transporters are identified using the NCBI database for different fungal and plant species. Together with three homologues in bacteria and four in human, a phylogenetic tree was built based on their amino acid sequences using the maximum-likelihood method in MEGA7.0 software. Clades corresponding to different subfamilies are denoted by different colours, with *A. thaliana* highlighted in green. Cr, C. reinhardtii; Pp, Physcomitrella patens; Sm, Selaginella moellendorffii; Mt, Medicago truncatula; Pt, Populus trichocarpa; Sl, Solanum lycopersicum; Os, Oryza sativa; Bd, Brachypodium distachyon; Sb, Sorghum bicolor.

levels of external Mg²⁺, mgr2 and mgr3 were comparable to the wild type (Supplementary Fig. 9). We also generated mgr1 mgr3 and mgr2 mgr3 double mutants lacking detachable transcripts of each gene (Supplementary Fig. 10a). Double mutant mgr1 mgr3 exhibited

Green alga

similar Mg sensitivity to that of single mutant *mgr1*, whereas that of *mgr2mg3* was comparable to the wild type under all conditions tested (Supplementary Fig. 10b,c). These results suggested that MGR1 functions as a major component in vacuolar Mg²⁺

Plant clade I

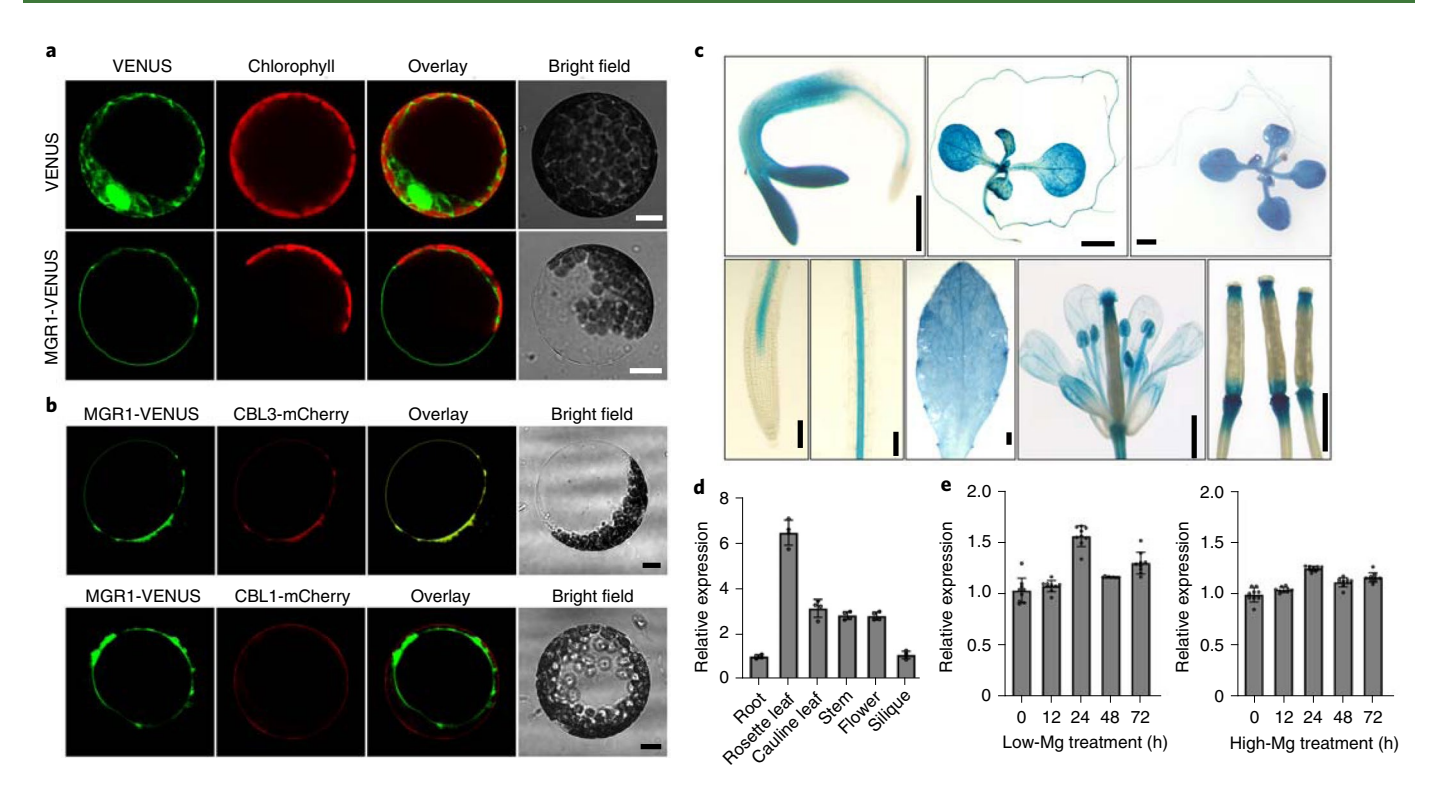


Fig. 3 | Subcellular localization and expression pattern of MGR1 in *Arabidopsis*. **a**, Confocal microscopy analysis of fluorescence signals from *Arabidopsis* protoplasts transiently expressing MGR1-VENUS fusion or VENUS alone, as indicated. Different panels show VENUS signal (green), chlorophyll autofluorescence (red), overlay and bright-field images from the same cell. Scale bars, 10 μm. More than ten independent cells were observed, with similar results. **b**, Colocalization of MGR1-VENUS with a tonoplast marker (CBL3-mCherry, top) but not with the plasma membrane marker (CBL1-mCherry, bottom). Scale bars, 10 μm. More than ten independent cells were observed with similar results. **c**, Expression patterns of *MGR1* promoter-driven *GUS* reporter in transgenic *Arabidopsis* plants at different developmental stages (top, from left to right: 2-, 6- and 10-day seedlings; scale bars, 2 mm) and in various adult tissues (bottom, from left to right: root tip, scale bar, 0.1mm; root elongation zone, scale bar, 0.1mm; rosette leaf, scale bar, 2 mm; flower, scale bar, 1 mm; siliques, scale bar, 1 mm). Six independent transgenic lines were analysed, with similar results. **d**, Quantitative PCR with reverse transcription (RT-qPCR) analysis of transcript levels of *MGR1* in different organs of *Arabidopsis* plants. Relative expression was double normalized against the housekeeping gene *ACTIN2* (AT3G18780) and expression level in the root. Data represent mean ± s.d. (*n* = 4). **e**, RT-qPCR analysis of transcript levels of *MGR1* under low- (left) and high-Mg (right) treatment. Relative expression was double normalized against the housekeeping gene *ACTIN2* and control expression values that were measured at 0 h. Data represent mean ± s.d. (*n* = 9).

sequestration in *Arabidopsis*, presumably due to its dominant expression over the other two homologues (Supplementary Fig. 10d). Therefore, we focused on functional analysis of MGR1 in subsequent studies.

The growth of *mgr1* mutant plants was inhibited by elevated Mg²⁺ levels in a dosage-dependent manner, as reflected by shorter roots, reduced fresh weight and lower chlorophyll content (Supplementary Fig. 11). This growth inhibition was specifically associated with high-Mg²⁺ toxicity because *mgr1* was sensitive to all Mg²⁺ salts tested, but not to any other metal ion in the medium (Supplementary Fig. 12). We extended phenotypic analysis to post-germination assays. When grown on 1/6 Murashige and Skoog (MS) medium (containing 0.25 mM Mg²⁺) for 2 weeks, the height of *mgr1* mutant plants was comparable to that of the wild type (Fig. 5a). However, after transfer to medium with elevated Mg²⁺ levels, *mgr1* mutants became severely stunted even in the presence of a moderate Mg²⁺ concentration (2 mM) that enhanced the growth of wild-type plants (Fig. 5a,b). In soil containing 60–100 mg kg⁻¹ Mg, *mgr1* plants were also stunted with necrosis at the leaf tips (Supplementary Fig. 13).

We grew both wild-type and mgr1 plants in hydroponic culture to monitor their response to Mg^{2+} concentrations. In the solution of $1/6\,MS$ salts (containing $0.25\,mM$ Mg^{2+}), mgr1 mutant plants were healthy and comparable to wild type (Fig. 5c). The addition of $5\,mM$ Mg^{2+} to the $1/6\,MS$ solution severely inhibited the growth of mgr1

plants (Fig. 5d,e), resulting in leaf tip necrosis and lower chlorophyll content (Fig. 5f). Under 10 mM external Mg²⁺, although wild-type plants were also stressed and stunted, *mgr1* plants became bleached and eventually died (Fig. 5c).

The mgr1 mutant (GK-322H07) harboured a tDNA insertion in the fifth exon of gene MGR1 (AT4G14240), as confirmed by DNA sequencing of the genomic locus (Supplementary Fig. 13c). While no full-length transcript of MGR1 was detectable in this mutant, nearby gene MGR2 (AT4G14230) appeared to be properly expressed as in the wild type (Supplementary Fig. 13d). To confirm that the tDNA insertional allele caused high-Mg sensitivity of the mgr1 mutant, we carried out a complementation test using a MGR1-containing genomic fragment. Indeed, transgenic expression of MGR1 in the mutant background restored MGR1 expression and fully rescued plant growth under high-Mg conditions, as well as in soil (Supplementary Fig. 14), demonstrating that MGR1 is critical for high-Mg tolerance in plants. Moreover, when we expressed the MGR1-GFP fusion in the mgr1 mutant background it also fully rescued the high-Mg-hypersensitive phenotype of mgr1 (Supplementary Fig. 15), suggesting that the MGR1-GFP fusion as used in our study, like native MGR1, is fully functional in planta and thus reflects correct subcellar localization in the tonoplast.

To understand how MGR1 regulates Mg²⁺ homeostasis in plants, we measured Mg content in *mgr1* and wild-type plants. When grown

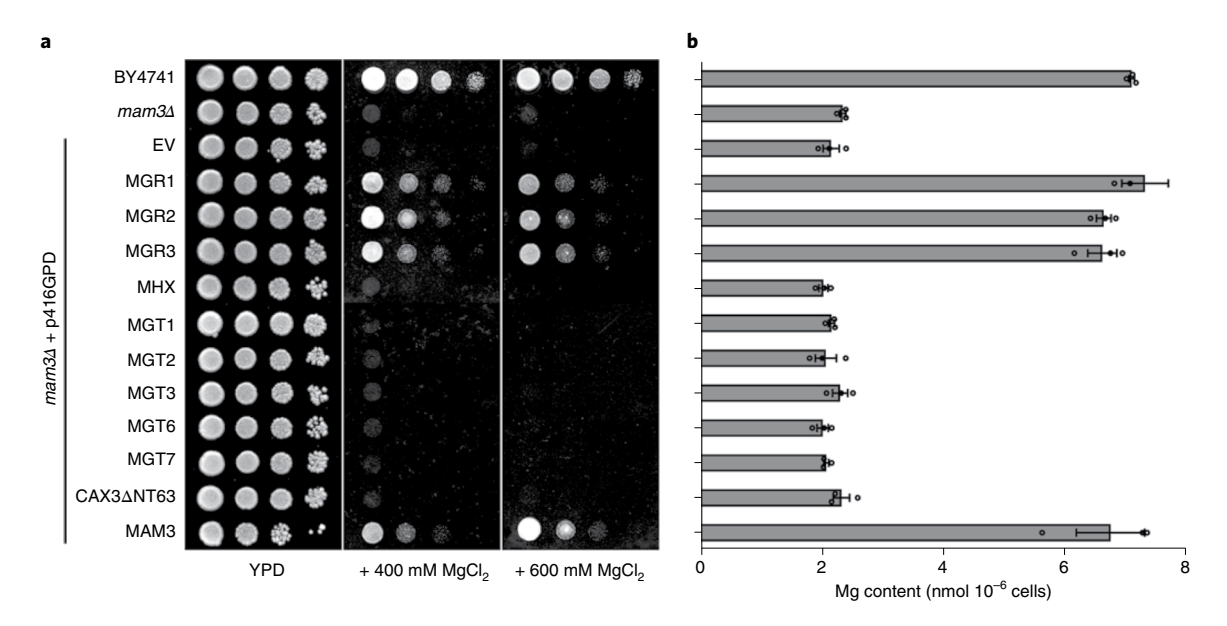


Fig. 4 | Expression of *Arabidopsis* vacuolar MGRs restores high-Mg tolerance of the yeast strain $mam3\Delta$ deficient in vacuolar Mg²+ sequestration. **a**, Complementation of $mam3\Delta$ by various plant transporters under high Mg²+ concentrations. Yeast cells of wild type (BY4741), $mam3\Delta$ and $mam3\Delta$ transformed with various genes in the p416GPD vector were spotted onto either YPD medium or YPD medium supplemented with 400 or 600 mM MgCl₂ in serial decimal dilutions. Plate cultures were incubated at 28 °C and photographed after 3 d. Each experiment was repeated using six independent clones, with similar results. CAX3 Δ NT63, truncated Ca²+/H+ exchanger CAX3 lacking N-terminal 63 amino acids resulting in constitutive activity in Ca²+ transport. **b**, Total cellular Mg content of various yeast strains, as indicated in **a**. Yeast cultures were grown in liquid SC medium containing 4 mM Mg²+, and cell-associated Mg content was analysed using ICP-OES. Data represent means \pm s.e.m. from three independent experiments.

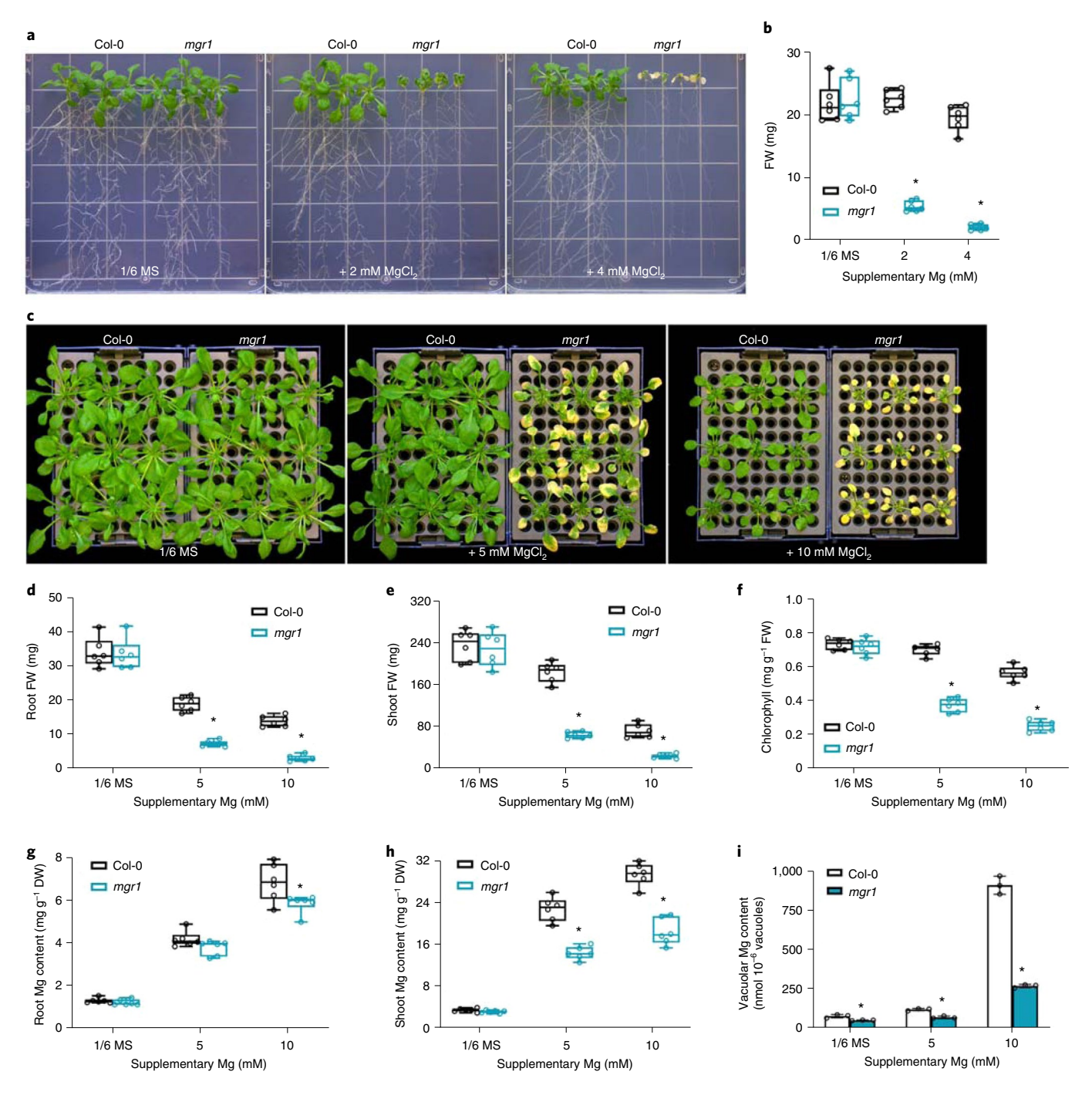
on 1/6 MS medium, *mgr1* and wild-type seedlings contained a comparable level of Mg (Supplementary Fig. 16). However, in the presence of an additional 2 mM or 4 mM MgCl₂ in the medium on agar plates, Mg content in *mgr1* seedlings was significantly lower than in wild-type samples (Supplementary Fig. 16). Importantly, the alteration in ionic profile was very specific to Mg because levels of other major cationic elements (including K, Ca, Na, Mn and Zn) in the *mgr1* mutant were comparable to the those in the wild type under all conditions tested (Supplementary Fig. 16). We also examined Mg content in different parts of plants under hydroponic culture. With increasing concentrations of external Mg²⁺, plants accumulated the majority (around 80%) of this element in shoot tissues (Fig. 5g,h). However, compared with wild-type plants, *mgr1* shoots retained much less Mg under high-Mg conditions (Fig. 5h), suggesting that shoot accumulation of Mg²⁺ was impaired in *mgr1* mutants.

To further address the role of MGR1 in vacuolar Mg²⁺ sequestration, we purified intact vacuoles from wild-type and mgr1 leaf mesophyll cells. Measurements of Mg content in the vacuolar lumen indicated that wild-type vacuoles displayed a high capacity for Mg²⁺ accumulation, as evidenced by a tenfold elevation in vacuolar Mg as external Mg²⁺ increased from basal (1/6 MS, 0.25 mM) and moderate (1 mM) to a high level (5 mM). In contrast, mgr1 mutant vacuoles accumulated much less Mg2+ (about 1/3) as compared to wild-type vacuoles (Fig. 5i) from plants treated with high external Mg²⁺ (5 mM). These data suggest that mgr1 is compromised in vacuolar Mg2+ sequestration, particularly under high Mg2+ concentrations. Together with tonoplast localization and functional assay in both the yeast model and the high-Mg²⁺-hypersensitive mgr1, our data support the conclusion that *Arabidopsis* MGR1, like yeast MAM3, functions as an essential transporter responsible for vacuolar Mg²⁺ sequestration.

Discussion

In the fungal model budding yeast, we provided several lines of evidence to support the mediation by MAM3 of vacuolar Mg^{2+}

sequestration. In parallel, an ACDP homologue from Arabidopsis (referred to as MGR1) proved to be critical for Mg²⁺ accumulation and high-Mg tolerance in plants. Because Arabidopsis MGR1 functionally substituted for MAM3 in the yeast model, we conclude that Mg²⁺ sequestration into the vacuole of fungal and plant cells works through an evolutionarily conserved mechanism that involves the same family of transporters. Interestingly, while plants appear to have ACDPs localized to the plasma membrane, similar to their bacterial and animal counterparts, fungal species possess only one ACDP member exclusively targeted to the vacuolar membrane. This phylogenetic pattern suggests that prokaryotes extrude Mg²⁺ as the major mechanism for detoxification under high-Mg conditions²⁹, whereas plants and fungi have evolved a more sophisticated mechanism utilizing the vacuolar store to buffer cytoplasmic Mg²⁺ status. Plasma membrane ACDP members in multicellular organisms, such as land plants and animals, may also play a role in intercellular (and long-distance) transport of Mg2+ throughout the body, in addition to extrusion and detoxification functions. The fact that fungi lack plasma membrane ACDPs suggests that Mg²⁺ partitioning into the vacuolar compartment may be adopted as a dual-functional mechanism in coping with both high (by detoxification) and low (by remobilization) external Mg2+. In this context, a CorA-type Mg2+ transporter, MNR2, residing in the yeast tonoplast is shown to mediate Mg2+ efflux from vacuole to cytoplasm17. Indeed, our genetic analysis further showed that MAM3 is epistatic to MNR2 in yeast, supporting the notion that Mg2+ accumulation into the vacuole pool (via MAM3) is a prerequisite for its subsequent retrieval (by MNR2). Nevertheless, it should be noted that loading of a specific ion into the vacuole may pass through more than one transport system, as exemplified by vacuolar Ca2+ partitioning through both Ca²⁺/H⁺ antiporters and Ca²⁺ pumps in yeast and plants^{35,36}. Hence we cannot exclude the possibility that other transporters, in addition to ACDPs, may also be involved in vacuolar sequestration. Considering the primary importance in maintaining Mg²⁺ homeostasis and their tonoplast localization in both yeast and plant cells,



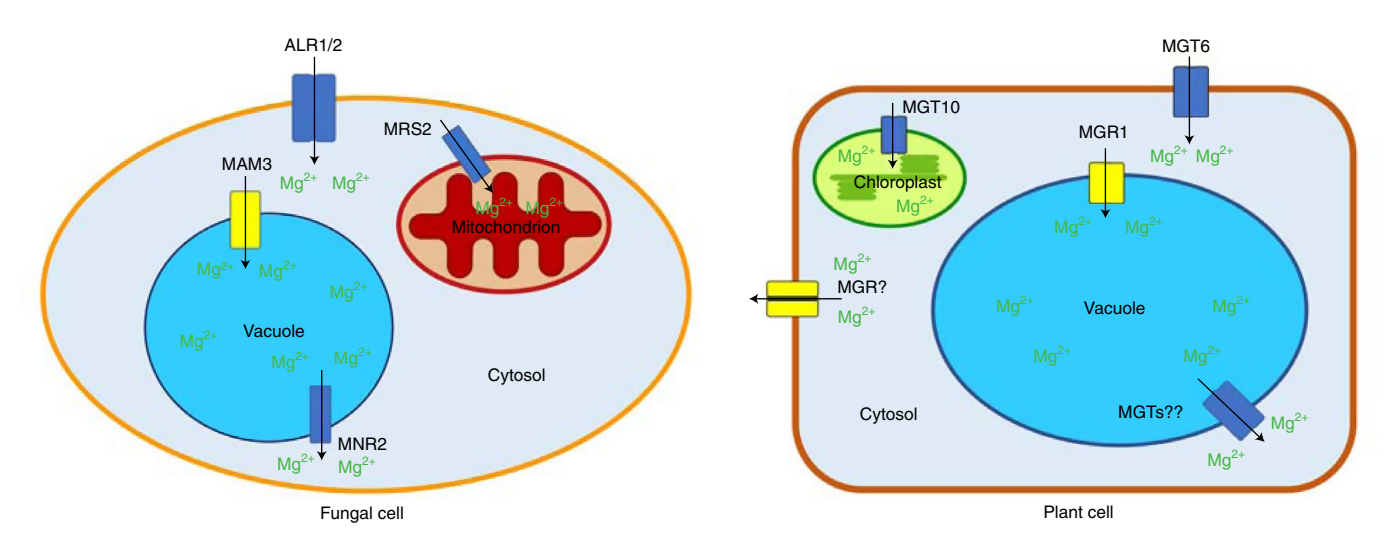


Fig. 6 | Model for Mg²⁺ transport network in a typical fungal cell and a typical plant cell. In general, CorA-type Mg²⁺ transporters (ALR1/2 and MRS2 in yeast, MGT6, MGT10 and unknown tonoplast MGTs in plants (blue) mediate Mg²⁺ uptake into metabolically active sites in the cell, including cytoplasm, mitochondrion and chloroplast. By contrast, ACDP-type transporters in the tonoplast, including MAM3 in yeast and MGR1 in plants (yellow), mediate Mg²⁺ sequestration into the vacuole, which functions as a conserved mechanism to detoxify excess Mg²⁺ in the cytoplasm. Plants have additional ACDP-type transporters (MGRs) in the plasma membrane that probably mediate Mg²⁺ efflux. Equivalent to MNR2 in yeast, unidentified CorA-type transporters (MGTs) in the plant cell tonoplast are proposed to be responsible for Mg²⁺ retrieval from the vacuolar store. These two conserved types of Mg²⁺ transporter coordinate to maintain Mg²⁺ homeostasis in fungal and plant cells in response to fluctuations in environmental Mg²⁺ supply.

we conclude that vacuolar ACDPs, as represented by yeast MAM3 and *Arabidopsis* MGR1, serve as a major and indispensable component required for Mg²⁺ translocation into the vacuole.

The soil content of Mg2+ varies widely depending on soil type, making Mg2+ homeostasis particularly important for plant growth and thus crop production. Even in soil types with a normal range of Mg²⁺, vacuolar sequestration may be critical for plant growth as indicated by the finding in this study that mgr1 mutant plants were severely stunted in regular soil. Extremely high levels of Mg²⁺ can be found in serpentine soils, imposing a serious stress on plant growth¹⁰. Under such stress conditions, vacuolar Mg²⁺ sequestration capacity must be enhanced to adapt to the environment. We previously established a Ca2+-dependent signalling pathway that enables plants to survive high-Mg conditions^{11,37}. Two tonoplast-associated calcineurin B-like (CBL) proteins are presumed to sense the specific Ca2+ signal elicited by high-Mg2+ stress which, in turn, recruits and activates a quartet of CBL-interacting protein kinases (CIPKs) to activate vacuolar Mg²⁺ sequestration¹¹. With the discovery of MGR1 as a vacuolar Mg2+ influx transporter, future studies should test the possibility that MGR1 may serve as a direct target for the vacuolar CBL-CIPK pathway in boosting plant tolerance to high-Mg conditions. On the other hand, the plasma membrane Mg²⁺ transporter MGT6 also serves as an indispensable component contributing to plant tolerance to high-Mg²⁺ stress, through a shoot-based mechanism²¹, suggesting that Mg²⁺ loading into shoot cells by MGT6 may be a prerequisite for subsequent Mg²⁺ sequestration into the vacuole by MGR1.

Animal cells contain several ACDP homologues in the plasma membrane, where they function in facilitating Mg²+ efflux²6-28. Prokaryotic ACDP homologues such as CorB, CorC and MpfA are also associated with cellular Mg²+ homeostasis²9,38. In line with these studies in animals and bacteria, our results on vacuolar ACDPs have not only advanced understanding of Mg²+ homeostasis in fungi and plants, but have also provided further support to the general notion that ACDPs may function as highly conserved Mg²+ transporters in all organisms ranging from bacteria to humans. However, when we attempted to measure MGR1 activity by electrophysiological approaches, no electrical currents were detected in multiple model

systems, implying that the transport process via MGR-type transporters is either electrically neutral or requires specific conditions and/or cofactors to become active. Further assays are required to define the transport mechanism of plant MGR proteins as well as ACDPs in other organisms.

In addition to ACDP-type transporters, CorA-type Mg²⁺ transporters are also highly conserved in all organisms ranging from bacteria, fungi and plants to animals. Interestingly, both types of transporter contain only a few transmembrane domains that might constitute a specific pore structure for Mg²⁺ transport. While CorA protein forms a pentamer with 'cone-shaped' channel features^{39,40}, the structure of ACDPs remains to be resolved. We propose that CorA- and ACDP-type transporters may facilitate opposite Mg²⁺ fluxes across cell membranes, with CorA acting in Mg2+ uptake and ACDP mediating the release of Mg²⁺ away from the cytoplasm, either to the extracellular space or into the vacuolar compartment. Taking the results from this report and earlier studies, we provide a model to illustrate the conserved mechanisms of Mg²⁺ transport in fungal and plant cells (Fig. 6). A universal concept for nutrient homeostasis may be derived from this model, in which diverse transporters form a complex transport network charging influx and efflux of the same ionic substrate to establish nutrient homeostasis for cell growth in the face of environmental fluctuations.

Methods

Yeast strains, growth media and general methods. Saccharomyces cerevisiae strain BY4741 (MATa, $leu2\Delta$, $met15\Delta$, $ura3\Delta$, $his3\Delta$) was used as a wild-type strain in most cases of this study. To construct the $mam3\Delta$ mutant, the homologous recombination-based gene deletion approach was employed in the background of BY4741. The gene deletion cassette mam3::LEU2, containing around 42-base-pair homology to the upstream and downstream of the MAM3 open reading frame, was amplified by PCR using plasmid p415GPD4 as a template (primer sequences available in Supplementary Table 1). The resulting DNA fragment was transferred into BY4741 cells using the PEG/LiAc method, and transformants were selected on SD-Leu medium. Several independent clones were picked and MAM3 gene deletion was verified by PCR analysis. For the analysis of double mutants, strains DY1514 and $mnr2\Delta$ were employed as described in a previous study¹⁷. The same gene deletion procedure was carried out in the background of both DY1514 and $mnr2\Delta$ to generate either an isogenic $mam3\Delta$ mutant or a double mutant of $mnr2\Delta$ $mam3\Delta$. All gene deletions introduced were also confirmed by PCR analysis.

Yeast cells were routinely grown in YPD or SD medium with 2% glucose, and required auxotrophic amino acid supplementation. For most phenotypic assays, YPD medium supplemented with different salts was used as indicated in each experiment. For the assay specifically addressing the effect of Mg2+ or Ca2+ on the yeast growth phenotype, a commercial yeast nitrogen base mix lacking all Mg²⁺ and Ca2+ salts (Sunrise Science) was used, and different levels of MgCl2 and CaCl2 were added to the medium for adjustment to the final concentration of Mg2+ and Ca²⁺ as needed. In the ionomic analyses of yeast strains, yeast cells were grown in liquid SC medium with divalent cations added in the chloride form to give a final concentration of 0.5 mM Ca²⁺, 4 mM Mg²⁺, 50 μ M Fe²⁺, 100 μ M Mn²⁺, 100 μ M Zn²⁺, 20 μM Co²⁺ and 20 μM Cu²⁺. For the functional complementation test, the yeast vector p416GPD⁴¹ was employed to express various genes. Yeast cells of mam3Δ were transformed with the indicated gene expression constructs by the PEG/LiAc method and selected on SD-Ura medium. Mg²⁺ tolerance tests were performed with different genotypes grown on YPD medium supplemented with either 400 or 600 mM MgCl₂ for 2-3 d at 28 °C.

Measurement of Mg content and other elements in yeast. Yeast cells were harvested from cultures at the stage of exponential growth and washed three times with 1 mM EDTA-Na $_2$ pH 8.0, followed by two washes with double-distilled water. Cells were then resuspended in double-distilled water in an appropriate volume to a final concentration at optical density (OD $_{600}$) = 0.75–1.00. After recording the OD $_{600}$ of each sample (one unit of OD $_{600}$ = 3 × 10 7 yeast cells ml $^{-1}$), 5 ml of yeast cells was collected by centrifugation and added with 1 ml of ultrapure HNO $_3$ (Sigma-Aldrich). Digested samples were further diluted tenfold, and concentrations of Mg $^{2+}$ and other ions in solution were determined by inductively coupled plasma–optical emission spectrometry (ICP–OES; PerkinElmer).

Phylogenetic analysis of ACDPs. Nine sequences with significant homology to the S. cerevisiae MAM3 protein were identified by the BLAST tool in The Arabidopsis Information Resource (TAIR; https://www.arabidopsis.org), and designated as MGR1-9 based on the degree of identity (from high to low) with MAM3. Subsequently, using MGR1 as a query, further plant homologues were identified by searching for sequences in selected representative plant genomes in the NCBI protein database (http://blast.ncbi.nlm.nih.gov/) covering different stages in plant evolution. MAM3 homologues in diverse fungal species were also retrieved from the NCBI protein database. Together with three homologues in bacteria and four in humans, a phylogenetic tree containing a total of 88 positions was built based on amino acid sequences from all selected species using the maximum-likelihood method in MEGA7.0 software. Accession numbers of all proteins are listed in Supplementary Table 2.

Plant materials and general growth conditions. All wild-type, mutant and transgenic *Arabidopsis* lines used in this study were the Columbia-0 (Col-0) ecotype. Transfer DNA insertional mutant lines GK-322H07 (*mgr1*), SALK_011518 (*mgr2*), SALK_043304 (*mgr3-1*) and SALK_054701 (*mgr3-2*) were obtained from the *Arabidopsis* Biological Resource Center (ABRC). Homozygous mutations of each gene in the background of each mutant line were confirmed using a PCR-based genotyping approach. *Arabidopsis* seeds were surface sterilized and sown on solidified MS medium. After stratification at 4 °C for 2 d, Petri dishes were maintained at 22 °C for 7 d. One-week-old seedlings were transferred to soil for subsequent growth at 22 °C in a growth chamber with a short-day (8-h/16-h light/dark) photoperiod or in the greenhouse under a long-day (16/8-h light/dark) photoperiodic condition.

Phenotyping of *Arabidopsis* plants under different conditions. For the germination assay, seeds were surface sterilized with 0.5% sodium hypochlorite for 5 min, washed three times with double-distilled water and sown on either 1/6 MS medium (containing 1% sucrose pH 5.8, solidified with 0.8% agarose) or 1/6 MS medium supplemented with different concentrations of MgCl₂ or other salts as indicated in each experiment. After 2-day stratification at 4 °C, plates were vertically placed in a growth chamber at 22 °C. For the post-germination assay, seeds were first sown on MS medium solidified with 1% phytoagar (Caisson Labs). After germination, 5-day-old seedlings were transferred to 1/6 MS medium (containing 1% sucrose pH 5.8, solidified with 0.8% agarose) supplemented without or with different concentrations of MgCl₂. For phenotypic assay in hydroponics, 7-day-old seedlings were transferred to liquid solution containing 1/6 MS salts. After 2-week culture, plants were treated with solutions containing 1/6 MS salts plus different concentrations of MgCl₂.

Promoter–GUS fusion analysis and histochemical assay of GUS activity. For construction of MGR1 promoter-driven GUS transgenic lines, a promoter region of approximately 2.0 kb immediately upstream of the ATG start codon of MGR1 gene was amplified from Col-0 genomic DNA by PCR and verified by sequencing. The PCR fragment was cloned into the binary vector pCAMBIA 1381Z. The construct was introduced into the A. tume faciens GV3101 strain, which was thereafter used to transform A. thaliana by the floral dipping method 42 . At least ten independent transgenic lines were selected, and T2 generation seedlings were subjected to GUS assay. For histochemical analysis to detect GUS expression, plant materials were

incubated at 37 °C for 4h in staining buffer (100 mM sodium phosphate pH 7.0, 10 mM EDTA, 0.5 mM K3[Fe(CN)6], 0.5 mM K4[Fe(CN)6], 0.1% Triton X-100) supplemented with 0.5 mM 5-bromo-4-chloro-3-indolyl- β -D-glucuronide. To clear chlorophyll from green tissues, stained materials were incubated in 75% ethanol overnight and then kept in 95% ethanol.

Plant functional complementation. For complementation of the *mgr1* mutant, a 4.5-kb genomic fragment containing the *MGR1* coding region, as well as around 1.5kb of the 5'-flanking DNA upstream of the starting codon, was amplified by PCR from *Arabidopsis* genomic DNA. The PCR product was cloned into the binary vector pCAMBIA1300. After confirmation by sequencing, the construct was transformed into *A. tumefaciens* strain GV3101 and introduced into *mgr1* mutant plants by the floral dip method⁴². Seeds of transgenic plants were screened on MS medium supplemented with 25 mgl⁻¹ hygromycin. Resistant seedlings were transferred to soil and grown in the greenhouse for seed propagation. T3 homozygous transgenic plants were subjected to gene expression analysis and phenotypic assay, together with wild-type plants and *mgr1* mutants.

RNA isolation and reverse transcription PCR analysis. *Arabidopsis* seedlings grown on Petri dishes were harvested and ground to a fine powder in liquid nitrogen. Total RNA was extracted using TRIZOL reagent (Invitrogen) following the manufacturer's instructions. After treatment with DNase I (Invitrogen) to remove potential DNA contamination, complementary DNA was synthesized from RNA samples at 42 °C using SuperScript II reverse transcriptase (Invitrogen). The resulting cDNA products were used for PCR amplification or quantitative real-time PCR analysis with the gene-specific primers listed in Supplementary Table 1.

Protein subcellular localization. To determine the subcellular localization of Arabidopsis MGRs, the coding region of each protein was in-frame fused to green fluorescent protein (GFP) in the transient expression vector pA7-GFP. Fusion constructs were introduced into Arabidopsis mesophyll protoplasts prepared from rosette leaves by the polyethylene-glycol-mediated transformation procedure⁴³ A similar fusion was performed for MGR1-VENUS specifically, and also used for colocalization studies with mCherry-based tonoplast or plasma membrane markers. For stable expression, fusions MGR1-GFP, MGR2-GFP and MGR3-GFP were subcloned downstream of a 35 S promoter in the pCAMBIA 1300 binary vector, and the resultant constructs were transferred into A. tumefaciens strain GV3101. Arabidopsis plants were transformed using the floral dipping method42. Twenty independent transgenic lines were randomly selected, and protoplasts were prepared from transgenic lines for subcellular localization examination. Plant vacuoles from the protoplast were released by osmotic shock using 500 mM sorbitol. Different types of fluorescence in transfected protoplasts were imagined using an LSM 710 confocal laser scanning microscope and processed using ZEN 2012 software (Carl Zeiss).

Mg measurement in plant materials. Plant samples were harvested separately from the root or shoot tissues at the end of each phenotypic assay, and surface washed with double-distilled water for 30 s. Samples were then thoroughly dried in an oven at 80 °C. Dry matter was collected in 15-ml tubes and digested with 1 ml of ultrapure HNO $_3$ (Sigma-Aldrich) overnight in a water bath at 95 °C. Digested samples were diluted to the appropriate concentrations with double-distilled water, and Mg $^{2+}$ levels in the solution were determined by ICP-OES (PerkinElmer).

Vacuole isolation and vacuolar Mg measurement. Plant vacuoles were isolated and purified from *Arabidopsis* rosette leaves as previously described⁴⁴. Vacuole purity was monitored by microscopy. Isolated vacuoles were dried at 70°C for 3 d and then digested with concentrated HNO₃ (Sigma-Aldrich). Quantification of Mg was performed by NexION 300 ICP–mass spectroscopy (PerkinElmer).

Reporting Summary. Further information on research design is available in the Nature Research Reporting Summary linked to this article.

Data availability

Data supporting the findings of this study are available within the paper and its Supplementary Information files. All *Arabidopsis* genes involved in this study can be found at TAIR (www.arabidopsis.org), with the following accession numbers: MGR1 (AT4G14240), MGR2 (AT4G14230), MGR3 (AT1G03270), MGR4 (AT1G47330), MGR5 (AT5G52790), MGR6 (AT4G33700), MGR7 (AT2G14520), MGR8 (AT3G13070) and MGR9 (AT1G55930). Yeast gene information is available at The *Saccharomyces* Genome Database (www.yeastgenome.org) as follows: MAM3 (YOL060C) and MNR2 (YKL064W). Other sequences can be found on the NCBI database (https://www.ncbi.nlm.nih.gov/), with accession numbers listed in Supplementary Table 2.

Received: 29 January 2021; Accepted: 7 December 2021; Published online: 27 January 2022

References

- Karley, A. J., Leigh, R. A. & Sanders, D. Where do all the ions go? The cellular basis of differential ion accumulation in leaf cells. *Trends Plant Sci.* 5, 465–470 (2000).
- Okorokov, L. A., Lichko, L. P. & Kulaev, I. S. Vacuoles: main compartments of potassium, magnesium, and phosphate ions in *Saccharomyces carlsbergenis* cells. *J. Bacteriol.* 144, 661–665 (1980).
- Boller, T. & Wiemken, A. Dynamics of vacuolar compartmentation. Annu. Rev. Plant Phys. 37, 137–164 (1986).
- 4. Martinoia, E., Meyer, S., De Angeli, A. & Nagy, R. Vacuolar transporters in their physiological context. *Annu. Rev. Plant Biol.* **63**, 183–213 (2012).
- Martinoia, E. Vacuolar transporters companions on a longtime journey. Plant Physiol. 176, 1384–1407 (2018).
- 6. Tang, R. J. & Luan, S. Rhythms of magnesium. Nat. Plants 6, 742-743 (2020).
- Okorokov, L. A. et al. Free and bound magnesium in fungi and yeasts. Folia Microbiol. 20, 460–466 (1975).
- Shaul, O. Magnesium transport and function in plants: the tip of the iceberg. Biometals 15, 309–323 (2002).
- Hermans, C., Conn, S. J., Chen, J., Xiao, Q. & Verbruggen, N. An update on magnesium homeostasis mechanisms in plants. *Metallomics* 5, 1170–1183 (2013).
- Walker, R. B., Walker, H. M. & Ashworth, P. R. Calcium-magnesium nutrition with special reference to serpentine soils. *Plant Physiol.* 30, 214–221 (1955).
- Tang, R. J. et al. Tonoplast CBL-CIPK calcium signaling network regulates magnesium homeostasis in Arabidopsis. *Proc. Natl Acad. Sci. USA* 112, 3134–3139 (2015).
- Amalou, Z., Gibrat, R., Trouslot, P. & D'Auzac, J. Solubilization and reconstitution of the Mg²⁺/2H⁺ antiporter of the lutoid tonoplast from *Hevea brasiliensis* latex. *Plant Physiol.* 106, 79–85 (1994).
- Borrelly, G. et al. The yeast mutant vps5Delta affected in the recycling of Golgi membrane proteins displays an enhanced vacuolar Mg²⁺/H⁺ exchange activity. Proc. Natl Acad. Sci. USA 98, 9660–9665 (2001).
- Shaul, O. et al. Cloning and characterization of a novel Mg(²⁺)/H(⁺) exchanger. EMBO J. 18, 3973–3980 (1999).
- MacDiarmid, C. W. & Gardner, R. C. Overexpression of the Saccharomyces cerevisiae magnesium transport system confers resistance to aluminum ion. J. Biol. Chem. 273, 1727–1732 (1998).
- 16. Kolisek, M. et al. Mrs2p is an essential component of the major electrophoretic Mg²⁺ influx system in mitochondria. EMBO J. 22, 1235–1244 (2003).
- Pisat, N. P., Pandey, A. & Macdiarmid, C. W. MNR2 regulates intracellular magnesium storage in Saccharomyces cerevisiae. Genetics 183, 873–884 (2009).
- Li, L., Tutone, A. F., Drummond, R. S., Gardner, R. C. & Luan, S. A novel family of magnesium transport genes in *Arabidopsis. Plant Cell* 13, 2761–2775 (2001).
- Schock, I. et al. A member of a novel *Arabidopsis thaliana* gene family of candidate Mg²⁺ ion transporters complements a yeast mitochondrial group II intron-splicing mutant. *Plant J.* 24, 489–501 (2000).
- Tang, R. J. & Luan, S. Regulation of calcium and magnesium homeostasis in plants: from transporters to signaling network. *Curr. Opin. Plant Biol.* 39, 97–105 (2017).
- Yan, Y. W. et al. Magnesium transporter MGT6 plays an essential role in maintaining magnesium homeostasis and regulating high magnesium tolerance in *Arabidopsis. Front. Plant Sci.* 9, 274 (2018).
- Li, J. et al. Diel magnesium fluctuations in chloroplasts contribute to photosynthesis in rice. Nat. Plants 6, 848–859 (2020).
- Conn, S. J. et al. Magnesium transporters, MGT2/MRS2-1 and MGT3/ MRS2-5, are important for magnesium partitioning within *Arabidopsis thaliana* mesophyll vacuoles. *New Phytol.* 190, 583–594 (2011).
- 24. Wang, C. Y. et al. Molecular cloning and characterization of a novel gene family of four ancient conserved domain proteins (ACDP). *Gene* **306**, 37–44 (2003).
- de Baaij, J. H. et al. Membrane topology and intracellular processing of cyclin M2 (CNNM2). J. Biol. Chem. 287, 13644–13655 (2012).
- 26. Hirata, Y., Funato, Y., Takano, Y. & Miki, H. Mg²⁺-dependent interactions of ATP with the cystathionine-beta-synthase (CBS) domains of a magnesium transporter. J. Biol. Chem. 289, 14731–14739 (2014).
- Stuiver, M. et al. CNNM2, encoding a basolateral protein required for renal Mg²⁺ handling, is mutated in dominant hypomagnesemia. *Am. J. Hum. Genet.* 88, 333–343 (2011).
- 28. Yamazaki, D. et al. Basolateral Mg²⁺ extrusion via CNNM4 mediates transcellular Mg²⁺ transport across epithelia: a mouse model. *PLoS Genet.* **9**, e1003983 (2013)
- Armitano, J., Redder, P., Guimaraes, V. A. & Linder, P. An essential factor for high Mg(²⁺) tolerance of Staphylococcus aureus. Front. Microbiol. 7, 1888 (2016).

- Sinharoy, S. et al. A Medicago truncatula cystathionine-beta-synthase-like domain-containing protein is required for rhizobial infection and symbiotic nitrogen fixation. Plant Physiol. 170, 2204–2217 (2016).
- Schaffers, O. J. M., Hoenderop, J. G. J., Bindels, R. J. M. & de Baaij, J. H. F. The rise and fall of novel renal magnesium transporters. *Am. J. Physiol. Ren. Physiol.* 314, F1027–F1033 (2018).
- Funato, Y. & Miki, H. Molecular function and biological importance of CNNM family Mg²⁺ transporters. J. Biochem. 165, 219–225 (2019).
- Yang, M., Jensen, L. T., Gardner, A. J. & Culotta, V. C. Manganese toxicity and Saccharomyces cerevisiae Mam3p, a member of the ACDP (ancient conserved domain protein) family. Biochem. J. 386, 479–487 (2005).
- Schmidt, U. G. et al. Novel tonoplast transporters identified using a proteomic approach with vacuoles isolated from cauliflower buds. *Plant Physiol.* 145, 216–229 (2007).
- Cunningham, K. W. & Fink, G. R. Calcineurin inhibits VCX1-dependent H⁺/ Ca²⁺ exchange and induces Ca²⁺ ATPases in Saccharomyces cerevisiae. Mol. Cell. Biol. 16, 2226–2237 (1996).
- 36. Pittman, J. K. Vacuolar Ca(2+) uptake. Cell Calcium 50, 139-146 (2011).
- Tang, R. J., Wang, C., Li, K. & Luan, S. The CBL-CIPK calcium signaling network: unified paradigm from 20 years of discoveries. *Trends Plant Sci.* 25, 604–617 (2020).
- Gibson, M. M., Bagga, D. A., Miller, C. G. & Maguire, M. E. Magnesium transport in Salmonella typhimurium: the influence of new mutations conferring Co₂+ resistance on the CorA Mg²⁺ transport system. Mol. Microbiol. 5, 2753–2762 (1991).
- Eshaghi, S. et al. Crystal structure of a divalent metal ion transporter CorA at 2.9 angstrom resolution. Science 313, 354–357 (2006).
- Lunin, V. V. et al. Crystal structure of the CorA Mg²⁺ transporter. Nature 440, 833–837 (2006).
- Mumberg, D., Muller, R. & Funk, M. Yeast vectors for the controlled expression of heterologous proteins in different genetic backgrounds. *Gene* 156, 119–122 (1995).
- Clough, S. J. & Bent, A. F. Floral dip: a simplified method for Agrobacteriummediated transformation of Arabidopsis thaliana. Plant J. 16, 735–743 (1998).
- Yoo, S. D., Cho, Y. H. & Sheen, J. *Arabidopsis* mesophyll protoplasts: a versatile cell system for transient gene expression analysis. *Nat. Protoc.* 2, 1565–1572 (2007).
- Robert, S., Zouhar, J., Carter, C. & Raikhel, N. Isolation of intact vacuoles from *Arabidopsis* rosette leaf-derived protoplasts. Nat. Protoc. 2, 259–262 (2007).

Acknowledgements

We thank ABRC for provision of *A. thaliana* seed stocks, and C. W. MacDiarmid for gifting yeast strains DY1514 and *mmr2*\(\textit{L}\). This work was supported by the National Science Foundation (no. MCB-1714795 to S.L.), the Innovative Genomics Institute at the University of California-Berkeley and the National Natural Science Foundation of China (grant no.31770267 to W.-Z.L.). C.W. is partly sponsored by a Tang Distinguished Scholarship at the University of California-Berkeley.

Author contributions

R.-J.T., S.-F.M., W.-Z.L. and S.L. conceived the study and designed the experiments. R.-J.T. performed all experiments on yeast. R.-J.T., S.-F.M. and X.-J.Z. performed most of the molecular cloning and genetic work in plants. R.-J.T. and B.Z. carried out ion measurements. Y.Y. and F.-G.Z. assisted with subcellular localization and gene expression analysis. C.W. helped with phylogenetic analysis and preparation of some of the figures. A.-G.F. coordinated the project. R.-J.T. and S.L. wrote the manuscript. All authors discussed the results and commented on the manuscript.

Competing interests

The authors declare no competing interests.

Additional information

Supplementary information The online version contains supplementary material available at https://doi.org/10.1038/s41477-021-01087-6.

Correspondence and requests for materials should be addressed to Wen-Zhi Lan or Sheng Luan.

Peer review information *Nature Plants* thanks Jian Feng Ma, Enrico Martinoia and the other, anonymous, reviewer(s) for their contribution to the peer review of this work.

Reprints and permissions information is available at www.nature.com/reprints.

Publisher's note Springer Nature remains neutral with regard to jurisdictional claims in published maps and institutional affiliations.

© The Author(s), under exclusive licence to Springer Nature Limited 2022

nature research

Corresponding author(s):	Sheng Luan
Last updated by author(s):	Dec 1, 2021

Reporting Summary

Nature Research wishes to improve the reproducibility of the work that we publish. This form provides structure for consistency and transparency in reporting. For further information on Nature Research policies, see our <u>Editorial Policies</u> and the <u>Editorial Policy Checklist</u>.

_					
∠ ¹	トコ	t i	ict	1	\sim

For	all statistical analyses, confirm that the following items are present in the figure legend, table legend, main text, or Methods section.
n/a	Confirmed
	\square The exact sample size (n) for each experimental group/condition, given as a discrete number and unit of measurement
	A statement on whether measurements were taken from distinct samples or whether the same sample was measured repeatedly
	The statistical test(s) used AND whether they are one- or two-sided Only common tests should be described solely by name; describe more complex techniques in the Methods section.
\boxtimes	A description of all covariates tested
	A description of any assumptions or corrections, such as tests of normality and adjustment for multiple comparisons
	A full description of the statistical parameters including central tendency (e.g. means) or other basic estimates (e.g. regression coefficient) AND variation (e.g. standard deviation) or associated estimates of uncertainty (e.g. confidence intervals)
	For null hypothesis testing, the test statistic (e.g. <i>F</i> , <i>t</i> , <i>r</i>) with confidence intervals, effect sizes, degrees of freedom and <i>P</i> value noted <i>Give P values as exact values whenever suitable.</i>
\boxtimes	For Bayesian analysis, information on the choice of priors and Markov chain Monte Carlo settings
\boxtimes	For hierarchical and complex designs, identification of the appropriate level for tests and full reporting of outcomes
\boxtimes	Estimates of effect sizes (e.g. Cohen's d, Pearson's r), indicating how they were calculated
	Our web collection on <u>statistics for biologists</u> contains articles on many of the points above.
So	ftware and code
Poli	cy information about <u>availability of computer code</u>
Da	ata collection WINLAB32 was used to collect ICP-OES data; ZEN 2012 was used to collect fluorescence signals from the co-focal microscopy.

For manuscripts utilizing custom algorithms or software that are central to the research but not yet described in published literature, software must be made available to editors and reviewers. We strongly encourage code deposition in a community repository (e.g. GitHub). See the Nature Research guidelines for submitting code & software for further information.

Microsoft Excel in office 365 and GraphPad Prism 7.0 were used for calculation and statistical analysis of the data; Adobe Photoshop CC2018

Data

Data analysis

Policy information about availability of data

All manuscripts must include a data availability statement. This statement should provide the following information, where applicable:

was used for image assembly. MEGA7.0 was used to perform the phylogentic analysis.

- Accession codes, unique identifiers, or web links for publicly available datasets
- A list of figures that have associated raw data
- A description of any restrictions on data availability

The data that supports the findings of this study are available within the article and its Supplementary Information files or from the corresponding authors upon reasonable request. A data availability statement has been inlouded in the manuscript.

Field-specific reporting					
Please select the one below that is the best fit for your research. If you are not sure, read the appropriate sections before making your selection.					
∑ Life sciences	Behavioural & social sciences	Ecological, evolutionary & environmental sciences			
For a reference conv of the document with all sections, see nature com/documents/nr-reporting-summany-flat ndf					

Life sciences study design

All studies must disclose on these points even when the disclosure is negative.

Sample size

No statistical methods were used to predetermine sample sizes. The exact number of samples in each experiment was specified in the figure legends. In all cases, sample sizes were adequate as the results were reproducible between different experimental groups. Sample sizes were chosen based on the experiment subjects and the number of samples that was sufficient to address subsequent statistical analysis. Basically, all the samples that were subjected to experiments were included in the data analysis, which ensured sufficient biological and technical repetitions.

Data exclusions

No data were excluded.

Replication

All attempts to replicate the experiments were successful. Each experiment was repeated for at least three times with similar results obtained. Number of repeats in each experiment was provided in the figure legends.

Randomization

Plants of different genotypes were randomly positioned in the growth chamber or in the greenhouse. Randomization was not applied to ion measurement. But the samples of the ion measurement were from random-based experiments in the earlier steps and sample collection in ion measurement was blinded, and therefore, all the unknown factors were supposed to be evenly contributed to control the covariates.

Blinding

Experiments for ion measurement were blinded. One person collected the samples, and the other person performed ICP analysis without knowing the sample identity before final data analysis. Blinding was impossible in other experiments because the author who conducted the experiments also performed data acquisition and analysis.

Reporting for specific materials, systems and methods

We require information from authors about some types of materials, experimental systems and methods used in many studies. Here, indicate whether each material, system or method listed is relevant to your study. If you are not sure if a list item applies to your research, read the appropriate section before selecting a response.

Materials & experimental systems		Methods		
n/a	Involved in the study	n/a	Involved in the study	
\times	Antibodies	\boxtimes	ChIP-seq	
\times	Eukaryotic cell lines	\boxtimes	Flow cytometry	
\times	Palaeontology and archaeology	\boxtimes	MRI-based neuroimaging	
\boxtimes	Animals and other organisms			
\times	Human research participants			
\times	Clinical data			
\boxtimes	Dual use research of concern			